Pergamon

Int. J. Heat Mass Transfer. Vol. 37, No. 6, pp. 1013–1027, 1994

0017-9310/94 $6.00 + 0.00

0017-9310(93)E0003-T

Heat and mass transfer in a contaminated porous concrete slab with variable dielectric properties

W. LI and M. A. EBADIAN†

Department of Mechanical Engineering, Florida International University, Miami, FL 33199, U.S.A.

and

T. L. WHITE,‡ R. G. GRUBB§ and D. FOSTER‡

‡Fusion Energy Division; §Chemical Technology Division, Oak Ridge National Laboratory, Oak Ridge, TN 37831, U.S.A.

(*Received* 17 *May* 1993 *and in final form* 8 *September* 1993)

Abstract—The effect of temperature dependent dielectric properties on concrete decontamination and decommissioning using microwave technology is investigated theoretically in this paper. The concrete is treated as a porous material, which has residual water and air within the pores. A one-dimensional model of unsteady heat and mass transport in the porous concrete with temperature dependent dielectric properties is developed. Based on this model, temperature and pressure with different microwave frequencies are predicted, the effects of the temperature dependent dielectric properties on microwave power dissipation, the temperature and pressure distributions for different microwave frequencies, and the different microwave power intensities are analyzed in detail. Four available industrial microwave frequencies of 0.896, 2.45, 10.6 and 18.0 GHz are used in the analysis. As a result of the dielectric properties varying with temperature, the power dissipation also varies with the heating times. Comparing the results for both temperature dependent and constant dielectric properties reveals that the variation of dielectric permittivity with temperature must be considered in a theoretical model of the concrete decontamination and decommissioning process for a low microwave frequency ($f < 2.45$ GHz).

1. INTRODUCTION

CONCRETE has been widely used for purposes of construction and shielding in nuclear facilities, such as reactors, canyon buildings, hot cells, waste processing facilities, etc. After several years of operation, many of the facilities now have contaminated concrete floors and walls. In most cases, only a small layer of the concrete exposed to radioactivity is contaminated. Depending on the exposure history, the depth of this contaminated concrete layer can be up to several centimeters. At some stage, this contaminated concrete layer must be removed and disposed of, while the bulk of the concrete, however, can be recycled or disposed of as nonradioactive material. Currently, mechanical techniques are used worldwide for the concrete decontamination and decommissioning process. To a varying extent, all of the mechanical methods generate dust, gases, or waste water, and an enormous amount of secondary radioactive waste, such as dust and water, is generated during the process of concrete decontamination and decommissioning. Storage and the recycling of these secondary radioactive wastes also engender other problems and expense.

Some successful industrial applications of microwaves are for the thawing of frozen meat, the vulcanization of rubber, cooking bacon, and for drying pasta [1, 2], and in the past decade, microwave technology has been applied to process many dielectric materials [3]. One successful example of this application is the microwave processing of ceramics [4]. 'Concrete breaking by microwaves' first appeared as the subject of an experimental study by Watson [5]. More recently, much effort has been devoted to the development of techniques for removing radioactively contaminated concrete. Several groups, Yasunaka *et al.* [6] in Japan, Hills [7] in Europe, White *et al.* [8] and Li *et al.* [9, 10] in the United States, have begun developing the new processes that use this technology in the decontamination of concrete.

When the microwave field interacts with the material, energy is transferred from the field to the molecular bonds of the material causing these bonds to 'vibrate'. This energy is then dissipated as heat and transported within the material. Thereafter, this microwave power dissipation will induce a nonuniform temperature distribution, and cause a temperature peak under the concrete surface, which will result in evaporation of the residual water, creating steam under high pressure. The pressure and thermal stress distributions within the concrete will cause a layer of concrete to spall off.

Based on experiments reported in refs. [7, 8] and the theoretical analysis [9, 10], it is generally agreed that the spalling-off of concrete by applying microwave heating is due mainly to the steam pressure created by steam generation from the residual water

† Author to whom all correspondence should be addressed.

NOMENCLATURE

A	constant, $S_{1,0}\rho_{1,0}+(1-S_{1,0})\rho_{2,0}$
a_0, a_1, a_2	constant, equation (1)
B	constant $(1-S_{1,0})\rho_{3,0}$
b_0, b_1, b_2, b_3	constant, equation (2)
C_p	specific heat of the concrete [J kg^{-1} K^{-1}]
E_x	electric field [V m^{-1}]
E_0	wave amplitude of the initial electric field [V m^{-1}]
E^+, E^-	complex constants, equations (5) and (6)
F	function defined by equation (23)
f	microwave frequency [s^{-1}] [Hz]
H_y	magnetic field [A m^{-1}]
h	heat transfer coefficient [W m^{-2} K^{-1}]
j	imaginary number, $\sqrt{(-1)}$
K	hydro-permeability [m^2]
k	thermal conductivity [W K^{-1} m^{-1}]
k_{eff}	effective thermal conductivity [W K^{-1} m^{-1}]
L	thickness of the concrete [m]
N	number of divisions in the numerical calculation
P	pressure [Pa]
Q_0	microwave power intensity [W m^{-2}]
Q_d	microwave power dissipation [W m^{-3}]
q	dimensionless heat generation, equation (29)
R	universal constant [N m kg^{-1} K^{-1}]
r	complex constant determined by the dielectric properties, equation (7)
S	volume saturation
T	temperature [°C]
T_∞	ambient temperature [°C]
t	time [s]
V	migration velocity vector [m s^{-1}]
x, y, z	coordinates [m].

Greek symbols

Δh_v	evaporation enthalpy [J kg^{-1}]
Δm	evaporation rate [kg s^{-1} m^{-3}]
$\Delta\tau$	dimensionless time stepsize
ε_{air}	dielectric permittivity of air, 8.86×10^{-12} [F m^{-1}]
ε'	real part of the complex dielectric permittivity, or dielectric constant [F m^{-1}]
ε''	imaginary part of the complex dielectric permittivity, or dielectric loss [F m^{-1}]
ε''_{eff}	effective dielectric loss, $\varepsilon''+\sigma/\omega$ [F m^{-1}]
ε^*	complex dielectric permittivity, $\varepsilon'-j\varepsilon''_{eff}$ [F m^{-1}]
η	complex constant, equation (7)
θ	dimensionless temperature, $(T-T_\infty)/T_0$
λ	wavelength of the microwave [m]
μ	magnetic permeability [H m^{-1}], or viscosity [N s m^{-2}]
μ_{air}	magnetic permeability of air, $4\pi\times10^{-7}$ [H m^{-1}]
μ_{con}	magnetic permeability of concrete [H m^{-1}]
ξ	dimensionless coordinate, z/L
Π	dimensionless effective thermal conductivity, $k_{eff}/k_{eff,0}$
ρ	density [kg m^{-3}]
σ	electric conductivity [Ohm^{-1}]
σ_c	compressive strength of the concrete [Pa]
σ_t	tensile strength of the concrete [Pa]
τ	dimensionless time, $tk_{eff,0}/(\rho C)_0 L^2$
ϕ	concrete porosity
ω	relative humidity or angle frequency of the microwave, $2\pi f$ [rad s^{-1}].

Subscript

air	air
ave	time average
i	value at the ith node
max	maximum value
s	spall-off condition
sat	saturation
0	initial condition at $t=0$, or the solid phase
1	liquid phase
2	vapor phase
3	air phase.

Other

$\|E\|$	norm of the complex value, $\sqrt{(E\cdot E^*)}$.

within the relatively impermeable porous concrete. Steam generation, and therefore the pressure distribution, are directly related to heat and mass transfer within the porous concrete materials. Based on non-equilibrium thermodynamics, Luikov stated that under certain circumstances, both diffusion and convection in the vapor phase are primary mechanisms of heat and mass transfer. He concluded that the temperature in the porous system plays an important role in mass transfer and that the temperature gradient becomes a driving force along with the concentration gradient [11]. Harmathy derived a set of governing differential equations of moisture migration in porous media during the pendular state [12]. Huang *et al.* [13] extended the work of ref. [12] to the inclusion of the funicular state, and predicted temperature, moisture

concentration, and pressure profiles by different theoretical approaches. To describe the dynamic phenomena occurring in heated materials, Wei *et al.* [14] modified Whitaker's derivations [15] and applied his equations to the material with a simple model of microwave heating [16]. Recently, Li *et al.* [9] analyzed the unsteady temperature and pressure distribution within the porous concrete subjected to microwave heating. Based on their investigation, the amount of residual water in the concrete is very small and its effect on the thermal properties is neglected. In addition, it is assumed that dielectric properties are constant for all temperatures and microwave frequencies ranging from 0.896 to 18 GHz [9]. However, the measurement in ref. [17] has revealed that the concrete dielectric properties are strongly dependent on microwave frequency and temperature.

The objective of this paper is to analyze heat and mass transfer within porous concrete that is subjected to microwave heating while considering the temperature dependent dielectric properties, as well as to demonstrate the effect of the variation of the dielectric properties on the modeling. It is a well known fact that a small change in the dielectric properties will significantly affect the electromagnetic fields, therefore changing the microwave energy dissipation within the concrete. Variations in the heat dissipation also affect heat and mass transfer within the concrete. The major parameters affecting concrete spall-off are: microwave power intensity ($Q_{0,\mathrm{ave}}$), microwave frequency (f), and concrete porosity (ϕ). The effects of variation in the dielectric properties, especially the complex dielectric permittivity (ε^*) on the microwave power dissipation ($Q_{\mathrm{d,ave}}$), unsteady temperature and inner pressure distributions (T and P, respectively), maximum temperature and inner pressure ($T_{\max}$ and $P_{\max}$, respectively), and the spall-off time (t_s) for different microwave frequencies, and microwave power intensity are fully discussed.

2. THE DIELECTRIC AND THERMAL PROPERTIES

The problem of concrete decontamination and decommissioning is directly related to the electromagnetic fields and the temperature distribution within the concrete. Therefore, knowing the dielectric properties is essential for a theoretical prediction. An accurate evaluation of the microwave field, which determines microwave power dissipation within the porous concrete, is very important and crucial for the whole process. At the same time, the temperature variation will result in changes in the dielectric properties, which will, in turn, affect the microwave energy dissipation, thus affecting the variation of the temperature distribution.

Motivated by the potential effect of the dielectric properties variation with temperature on the decontamination and decommissioning process, the dielectric properties of concrete were experimentally measured [17] for different temperatures and microwave frequencies. Based on the following basic assumptions for concrete, the measured dielectric properties and other published thermal properties are applied to the present analysis.

2.1. *Basic assumptions*

2.1.1. *The homogeneous and isotropic porous medium.* Figure 1 is a set of photographs taken from a scanning electron microscope (JEOL LSM-35CF). It illustrates the micro-structure of the concrete used in ref. [8] for their experimental investigation. Concrete is basically a mixture of sand, aggregate, and cement, all of which contain pores. The large pores, shown in Fig. 1(a) (enlarged 26 times), are caused by incomplete compaction, while the fractures between the sand and the cement and the small pores within the cement, shown in Fig. 1(b) (enlarged 800 times), are created by cement bleeding. These voids may occupy from a fraction of the volume up to 20% of the whole volume of the concrete. Generally, concrete is a multi-phase porous medium in which liquid, vapor, and residual air initially exist. In this study, a rigid, non-deformable solid concrete matrix is considered. In a macroscopic sense, the pore structure within the concrete is assumed to be homogeneous and isotropic. Therefore, a heat and mass transfer model for a homogeneous and isotropic porous medium is used in the current analysis.

2.1.2. *The local thermal equilibrium.* Based on the studies of concrete properties [18], the hydropermeability of the concrete is $\sim 7 \times 10^{-16}$ m^2, and the specific surface of the concrete is $\sim 4 \times 10^8$ m^{-1}. In the process of concrete decontamination and decommissioning, the concrete spall-off time is ~ 10 s. Therefore, the movement of vapor and air through the concrete is sufficiently slow, and the surface areas of all phases are sufficiently large. Thus, it is reasonable to assume that the local thermal equilibrium between all phases (water, steam, air, and the solid concrete matrix) is achieved instantaneously.

2.2. *The dielectric properties*

It is a well known fact that the concentration of ferromagnetic material in concrete is negligible. Hence, it can be assumed that the magnetic permeability of the concrete slab (μ_{con}) approximately equals the value of the air (μ_{air}), i.e. $\mu_{\mathrm{con}} \approx \mu_{\mathrm{air}}$. Classical methods of measuring the dielectric permittivity of a material require special preparation of a test sample that is placed inside a waveguide, or cavity. For simplicity of the test sample preparation and temperature control, a newly developed, open-ended coaxial line technique is used for measuring the concrete dielectric properties. However, the relation between the measured reflection coefficient and the complex permittivity is complicated. Several attempts and improvements have been made to clearly determine

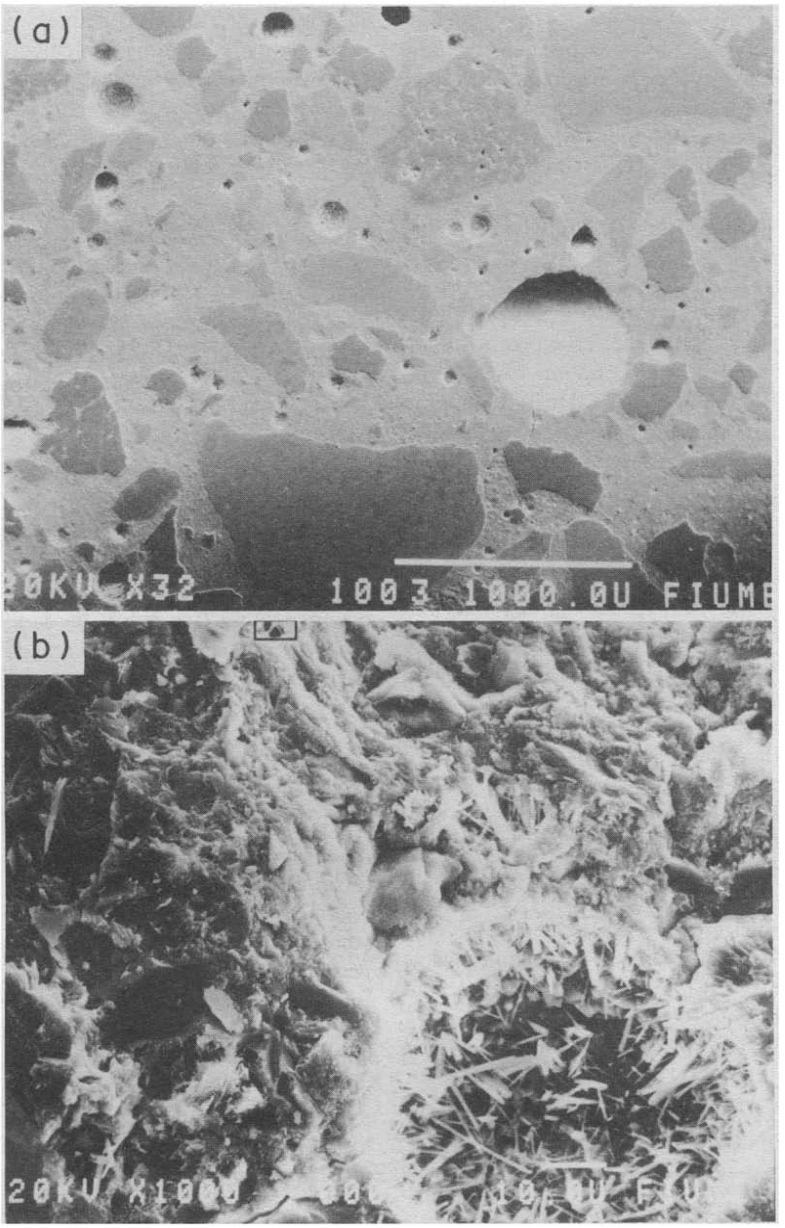

FIG. 1. Microstructure of concrete. (a) 26 times actual size; (b) 800 times actual size.

the dielectric permittivity from the measured data [19, 20]. The formulations described in ref. [20] are employed in our measurement.

For measuring the dielectric permittivity of concrete, a desired microwave signal was obtained using a dielectric probe kit (HP-85070A). The incident and reflected signal outputs of the transmission-reflection test set (HP-85047A) are coupled to a network analyzer (HP-8510B) and to a personal computer through an HP-IB instrument (HP-82335A). The size of the test sample is $2\times2\times2$-in.^{3}. The sample is placed in a heating oven (OMEGA P-750), which has power up to 9 kW. The effect of the moisture variation within the concrete on the dielectric properties is assumed to be negligible. Thus, it is assumed that the phase change within the concrete does not affect the concrete dielectric properties, and that these properties are a function of frequency and temperature only. The final results are formulated according to the following relations:

$$\frac{\varepsilon'}{\varepsilon_{\text{air}}} = a_0(f)+a_1(f)T^{a_2(f)} \tag{1}$$

$$\frac{\varepsilon''_{\text{eff}}}{\varepsilon_{\text{air}}} = b_0(f)+b_1(f)T+b_2(f)T^2+b_3(f)T^3, \tag{2}$$

where T is the temperature (°C) and $a_0, a_1, a_2, b_0, b_1, b_2$ and b_3 are constants regressed from the measurement [17].

The measured dielectric constant (ε') and the effective dielectric loss ($\varepsilon''_{\text{eff}}$) are plotted in Fig. 2. The measurements by Hasted and Shah [21] for water content of approximately 0.1 ($\phi S_1 = 0.1$) are also indicated in the figure. For their measurements, the temperature was controlled at $20 \pm 1.0°C$, while in our measurement, the temperature was varied from room temperature ($\sim 25°C$) to 250°C. It shows that our measurements agree well with the previous investigations.

2.3. *The thermal properties*

The liquid and vapor are categorized as pure water and water steam, respectively. The properties of the pure water and the steam documented in refs. [22, 23] are applied in the computation. Air is treated as the ideal gas in the whole process. It is further assumed that there is no chemical reaction during the process, i.e. there is no generation of air and other chemical components.

3. PROBLEM FORMULATION

3.1. *The microwave field and the microwave energy dissipation*

Microwaves are electromagnetic waves having frequencies from 300 MHz to 300 GHz. Therefore, microwaves satisfy Maxwell's equation, which

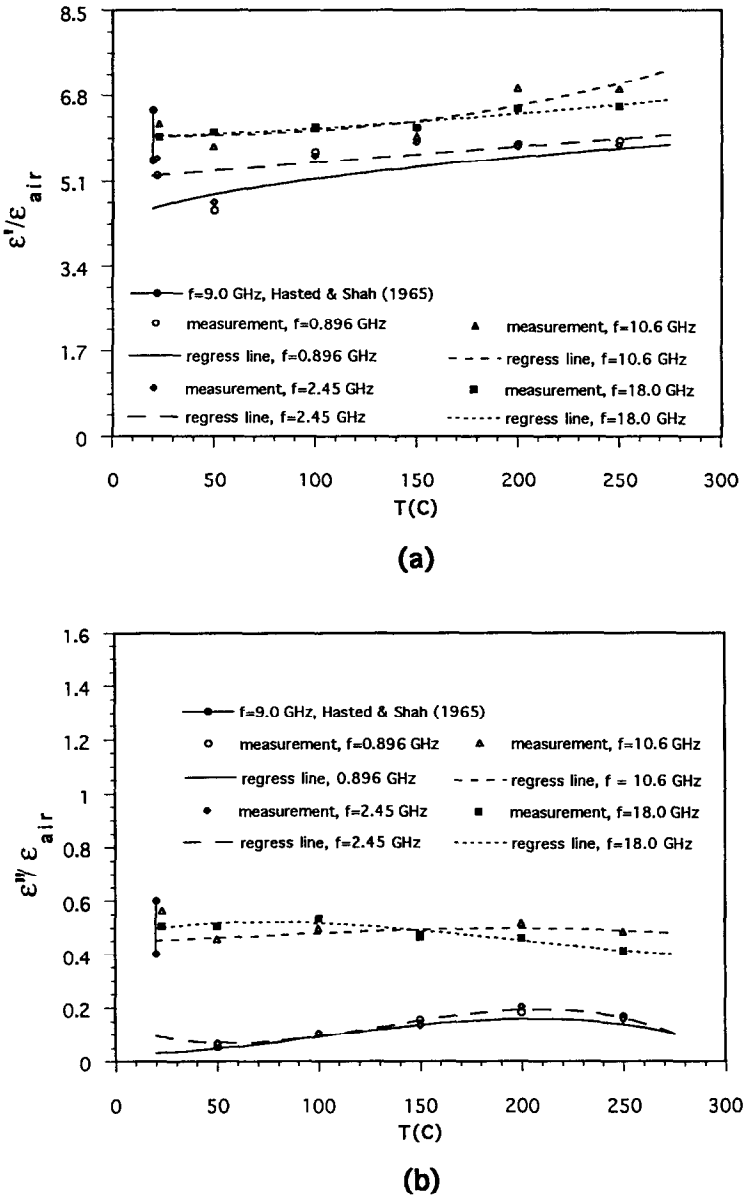

FIG. 2. Variation of concrete dielectric permittivity ($\varepsilon^* = \varepsilon' - j\varepsilon''_{\text{eff}}$) with temperature. (a) Variation of dielectric constant (ε'); (b) variation of effective dielectric loss ($\varepsilon''_{\text{eff}}$).

describes the electromagnetic fields. In a macroscopic sense, one can now consider an electrically homogeneous concrete slab with a front surface at $z = 0$ directly exposed to the microwave source, Fig. 3(a). The concrete slab is further divided into N subdivisions, and the complex dielectric permittivity, ε^* ($\varepsilon' - j\varepsilon''_{\text{eff}}$) is assumed to be uniform in this small subdivision and a function of the local temperature and the microwave frequency only.

The governing equation for the electromagnetic

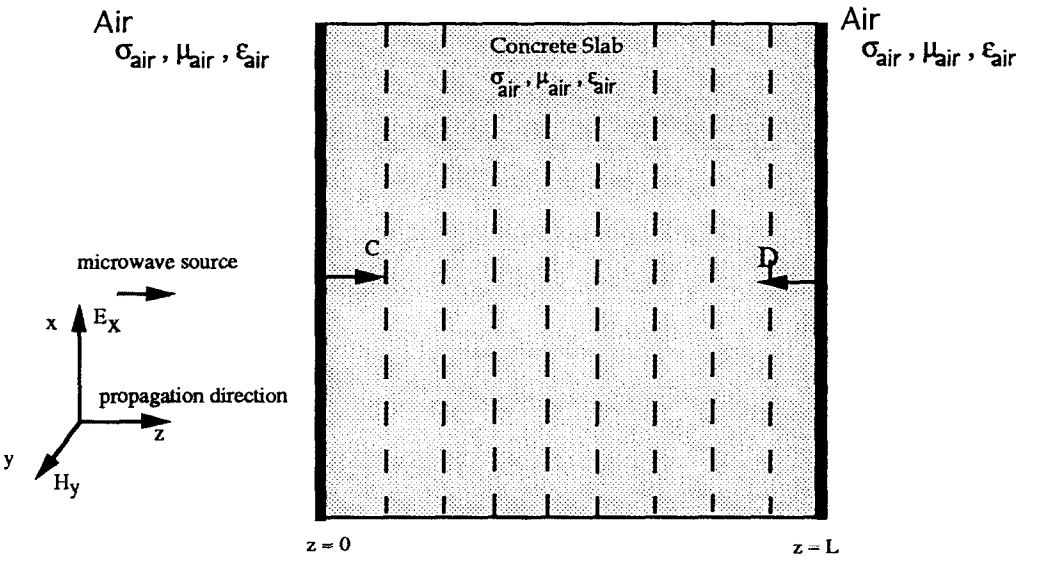

(a)

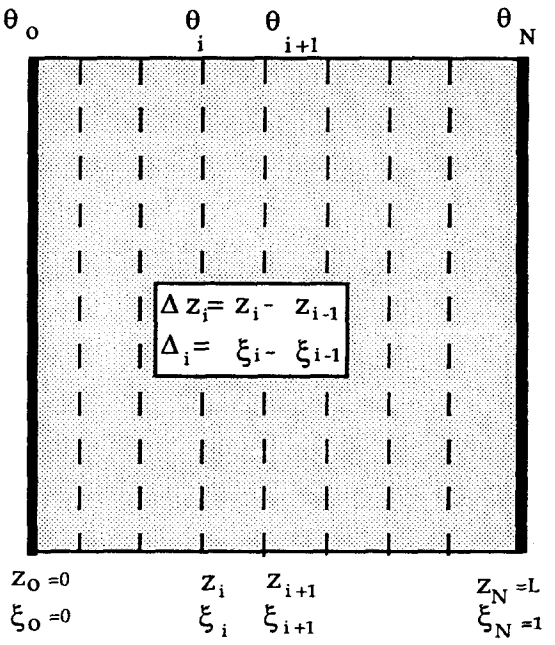

(b)

FIG. 3. Geometry and coordinates of the concrete slab. (a) Geometry of the concrete slab; (b) geometry of the numerical nodes.

fields in each subdivision can be simplified as follows for the plane wave [24, 25]:

$$\frac{dE_x^i}{dz} = -j\mu\omega H_y^i \tag{3}$$

$$\frac{dH_y^i}{dz} = -j\omega\varepsilon_i^* E_x^i, \tag{4}$$

with general solution as:

$$E_x^i = E_i^+ e^{-r_i z} + E_i^- e^{r_i z} \tag{5}$$

$$H_y^i = \frac{1}{\eta_i}(E_i^+ e^{-r_i z} + E_i^- e^{r_i z}) \tag{6}$$

in which

$$r_i = j\omega\sqrt{(\mu_{con}\varepsilon_i^*)} \quad \text{and} \quad \eta_i = \sqrt{(\mu_{con}\omega/\varepsilon_i^*)} \tag{7}$$

where E_i and H_i are the electric and magnetic field potential, and μ_{con} and ε_i^* are the magnetic permeability and complex dielectric permittivity at the ith division of the concrete, respectively. E_i^+ and E_i^- are the unknown constants to be determined by the boundary conditions, which can be numerically solved [24, 25]. Therefore, the electric and magnetic fields in each subdivision are calculated using equations (5) and (6). Since r_i and η_i, and E_i^+ and E_i^- are complex values, the final solution of E_x and H_y are also complex.

Finally, since the microwave frequencies are very high (from 300 MHz to 300 GHz), the time scale of the sinusoidal variations of the microwave field is much smaller than that of the temperature variations in the concrete. One can then separate the sinusoidal variation of the microwave from the unsteady heat transport phenomena. The time averaged microwave power dissipation ($Q_{d,ave}$) can thus be calculated as [9]:

$$Q_{d,ave}^i = \tfrac{1}{2}(\omega\varepsilon''_{eff,i})\|E_1^i\|. \tag{8}$$

It is noted that the time averaged microwave power dissipation ($Q_{d,ave}^i$) in the ith subdivision is proportional to the product of the imaginary section of the dielectric permittivity (ε''_{eff}) and the square of the norm of the complex electric potential (E_x^i), while both are strongly dependent on the local temperature.

3.2. *Heat and mass transfer within the concrete*

3.2.1. *The governing equations.* By conservation of mass, momentum, and energy in a porous medium, the governing equations of mass, momentum, and energy for the solid (0), liquid (1), vapor (2), and air (3) phases can be derived by using a volume (local) average technique. As indicated, the concrete spall-off time using microwave heating technology is ~ 10 s. The time for water and vapor or air moving between two consecutive wave peaks under a unit pressure gradient within the concrete slab ($\lambda\mu/K$) is about 8.6×10^7 s (2.4×10^4 h), where λ is the wavelength of the microwave in the concrete. Thus, the liquid, vapor, and air movement can be neglected as an approximation, and only the evaporation is considered. Therefore, the governing equations for a one-dimensional problem with concrete porosity, ϕ, can be further simplified to the following equations as [9]:

Mass conservation:

$$\phi\frac{\partial}{\partial t}(S_1\rho_1) + \Delta m = 0 \tag{9}$$

$$\phi\frac{\partial}{\partial t}[(1-S_1)\rho_2] - \Delta m = 0 \tag{10}$$

$$\frac{\partial}{\partial t}[(1-S_1)\rho_3] = 0. \tag{11}$$

Momentum conservation:

$$V_i = 0, \quad i = 1,2,3, \tag{12}$$

while the pressures of all the fluid phases can be determined by the state equation as the functions of temperature (T) and densities (ρ_i) only. Thus,

$$P_i = f_i(T,\rho_i), \quad i = 1,2,3. \tag{13}$$

Energy conservation:

$$(\rho C_p)_0\frac{\partial T}{\partial t} = \frac{\partial}{\partial z}\left(k_{eff}\frac{\partial T}{\partial z}\right) + Q_{d,ave}(T,z) - \Delta m\Delta h_v + \frac{\partial P_1}{\partial t}, \tag{14}$$

where

$$(\rho C_p)_0 = (1-\phi)\rho_0 C_{p,0} + \phi\sum_{i=1}^{3} S_i\rho_i C_{p,i} \tag{15}$$

$$k_{eff} = (1-\phi)k_0 + \phi\sum_{i=1}^{3} S_i k_i \tag{16}$$

$$S_2 = S_3 = 1 - S_1, \tag{17}$$

in which Δm is the evaporation rate during the heating process, ϕ is the porosity of the concrete system; S, ρ, and V are the volume saturation ratio, density, and migration velocity of the different phases, respectively. Volume saturation ratio, S, is defined as the fraction volume of each phase (liquid, 1, vapor, 2, and air, 3) in the void space. T is the equilibrium temperature, $C_{p,0}$ is the specific heat of the solid concrete, k and C_p are the thermal conductivity and specific heat for each phase, respectively. $Q_{d,ave}$ is the time averaged microwave power dissipation for all phases in the concrete, and Δh_v is the water evaporation enthalpy. Since $(1-\phi)\rho_0 C_{p,0}$ is dominant in $(\rho C_p)_0$, the variations resulting from the changes of S_i and ρ_i are insignificant. Therefore, the initial value of $(\rho C_p)_0$ is used in the calculation. Similar to $(\rho C_p)_0$, the initial value of k_{eff} is also used during the calculation.

3.2.2. *The constitutive state equations.* If the momentum equations are described as the state equations, there are four equations for heat and mass transfer in the concrete (three for continuity and one for energy) with six unknown parameters (1 volume saturation, 3 densities, 1 evaporation rate and 1 temperature), while

the vapor, air and liquid pressures are considered as dependent variables. Therefore, two more equations are needed to determine all of the parameters. From equilibrium thermodynamics, the pressure for each fluid phase has a certain relation with the corresponding density (ρ_i) and the equilibrium temperature (T). For the multi-phases in a porous medium, liquid pressure is assumed to be the same as tensile stress within the solid concrete without considering capillary pressure. This pressure equals the summation of the vapor and air pressures as:

$$P = P_1 = P_2 + P_3. \tag{18}$$

The concrete to be decontaminated is usually more than ten years old. Although the hydropermeability is very low, it might also initially be assumed that the vapor pressure (P_2) within the concrete is a function of the relative humidity around the concrete, which has the following relationship:

$$P_2 = \omega P_{\text{sat}}, \tag{19}$$

where ω is the relative humidity around the concrete. For simplicity, saturated vapor ($\omega = 1$) is used in the analysis. The residual water in the concrete subjected to microwave heating continuously evaporates. A fraction of the vapor phase is then almost dominant in the air–vapor mixture. Therefore, it is assumed that the vapor pressure equals the saturation pressure of the vapor, i.e. $P_2 = P_{\text{sat}}(T)$ throughout the entire process.

3.2.3. *The initial and boundary conditions.* The initial condition of all densities (ρ_i), the liquid volume saturation (S_1), the temperature (T), and the boundary condition of the temperature (T), must be known to solve the governing equations. The initial conditions are:

$$\rho_1 = \rho_{1,0}, \quad \rho_2 = \rho_{2,0}, \quad \rho_3 = \rho_{3,0}, \quad S_1 = S_{1,0}, \quad T = T_0 \quad \text{and} \quad P_1 = P_{1,0} \quad \text{at } t = 0, \tag{20}$$

where $P_{1,0}$ is the atmospheric pressure (101.3 kPa). All initial conditions should also satisfy the state equations at the initial temperature (T_0) and pressure ($P_{1,0}$).

Assuming constant wall temperatures are specified at both the front and back surfaces of the concrete, one can then clarify the following boundary conditions:

$$T = T_\infty, \quad \text{at } z = 0, L. \tag{21}$$

Precisely, the governing equations have four differential equations with three state equations and two pressure relations, which are nonlinear parabolic differential equations. Theoretically, with the specified initial and boundary conditions, they have unique solutions. Combining the continuity and energy equations for the liquid and vapor phases, and integrating with respect to time and using the initial conditions, one can obtain the following relation:

$$(\rho C_p)_0 F(T) \frac{\partial T}{\partial t} = \frac{\partial}{\partial z}\left(k_{\text{eff}} \frac{\partial T}{\partial z}\right) + Q_{\text{d,ave}}, \tag{22}$$

where $(\rho C_p)_0$ is the initial value of equation (15), and $F(T)$ is defined as:

$$F(T) = \frac{1}{(\rho C_p)_0}\left\{(\rho C_p) - \frac{\phi \Delta h_v}{(\rho_1 - \rho_2)^2}\left[\rho_1(A-\rho_1)\frac{d\rho_2}{dT} - \rho_2(A-\rho_2)\frac{d\rho_1}{dT}\right] - \frac{dP_1}{dT}\right\}, \tag{23}$$

in which

$$A = S_1\rho_1 + (1-S_1)\rho_2 = S_{1,0}\rho_{1,0} + (1-S_{1,0})\rho_{2,0}. \tag{24}$$

The volume saturation, S_1, air density, ρ_3, and the evaporation rate, Δm, can be obtained from the following relation:

$$S_1 = 1 - \frac{\rho_1 - A}{\rho_1 - \rho_2} \tag{25}$$

$$\rho_3 = \frac{\rho_1 - \rho_2}{\rho_1 - A} B, \tag{26}$$

and

$$\Delta m = -\phi \frac{\partial}{\partial t}(S_1\rho_1) = -\phi \frac{\partial}{\partial t}\left(\frac{A-\rho_2}{\rho_1-\rho_2}\rho_1\right) = \frac{-\phi}{(\rho_1-\rho_2)^2}\left[\rho_1(A-\rho_1)\frac{d\rho_2}{dT} - \rho_2(A-\rho_2)\frac{d\rho_1}{dT}\right]\frac{\partial T}{\partial t}, \tag{27}$$

where

$$B = (1-S_1)\rho_3 = (1-S_{1,0})\rho_{3,0}. \tag{28}$$

Note that $\partial P_1/\partial t = (dP/dT)(\partial T/\partial t)$. Combining equations (13) for the three phases, equations (18) and (19) and equation (26), a total of six equations, of all seven unknowns (pressures, densities and temperature), only one needs to be specified as independent, i.e. all pressures and densities can be specified as functions of T only. It is estimated that the maximum value of dP_1/dT is only 1.7% of the value of $(\rho C_p)_0$ within the temperature range from 25 to 250°C. Therefore, it is quite reasonable to neglect the term $(\partial P_1/\partial t)$ caused by the work done by pressure.

3.3. *Dimensionless equation and initial and boundary conditions*

By introducing the following dimensionless parameters and knowing that $T_\infty = T_0$,

$$\theta = \frac{T - T_\infty}{T_0}, \quad \xi = \frac{z}{L}, \quad \tau = \frac{k_{\text{eff},0}\, t}{(\rho C_p)_0 L^2}, \quad \Pi = \frac{k_{\text{eff}}}{k_{\text{eff},0}}, \quad q = \frac{Q_{\text{d,ave}}(T) L^2}{k_{\text{eff},0} T_0}. \tag{29}$$

The energy equation and the initial and boundary

conditions can be written in the following dimensionless form:

$$F(\theta)\frac{\partial\theta}{\partial\tau}=\frac{\partial}{\partial\xi}\left(\Pi\frac{\partial\theta}{\partial\xi}\right)+q(\theta,\xi), \tag{30}$$

$$\theta=0, \quad \text{at } \tau=0 \tag{31}$$

$$\theta=0, \quad \text{at } \xi=0 \text{ and } 1. \tag{32}$$

The method of lines (MOL) [26], which is similar to a procedure of using the finite difference method, is used to solve the above equation. To ensure that each wavelength of the microwaves in the concrete, $\lambda\approx 1/[f\sqrt{(\mu_{air}\varepsilon')}]\approx 6.3\times10^{-3}$ m for $f=18$ GHz, has more than 60 subdivisions in the numerical calculation, the total subdivision number of $N=6000$ is used in the analysis. To ensure convergence of the numerical solution, it should also satisfy the following criteria in our calculation:

$$\frac{\Delta\tau\Pi_i}{F(\theta_i)\Delta_i^2}\leqslant\tfrac{1}{2}. \tag{33}$$

An adaptive time stepsize ($\Delta\tau$) control technique with a fourth order Runge–Kutta method is used to achieve the convergence of the solution during the process of solving the transformed ordinary differential equations.

4. RESULTS AND DISCUSSION

The composition and the thermal properties of the concrete used in the analysis are shown in Table 1. The formulations used to calculate the thermal properties of water and steam are listed in Table 2. As a result of our previous study [9], the effect of porosity (ϕ) on the heat and mass transfer is very small since the microwave power level, or intensity ($Q_{0,ave}$), is very high. Therefore, a 5–10% difference in concrete porosity does not affect the temperature and pressure distributions, as well as the spall-off time. During the present analysis, only $\phi=0.1$ is used. In the present discussion, four commonly used frequencies, 0.896, 2.45, 10.6, and 18.0 GHz, are utilized based on industrial availability.

4.1. *Microwave power dissipation*

It is seen from equation (8) that the microwave power dissipation ($Q_{d,ave}$) is a product of the angular frequency ($\omega=2\pi f$), the effective dielectric loss (ε''_{eff}) and the square of the norm of the electric field (E_x). Both the effective dielectric loss and the electric field are functions of the temperature (T) for a specified microwave frequency (f). In Figs. 4(a) and (b), the dimensionless microwave power dissipations ($Q_{d,ave}L/Q_{0,ave}$) at different heating times within the concrete for frequencies of 0.896 and 2.45 GHz, respectively, are presented. For higher frequencies ($f=10.6$ and 18.0 GHz), variations of the average microwave power dissipation over two wavelengths are plotted in Figs. 4(c) and (d), since the wavelength for the higher frequencies is too small to plot. In these figures, *Case 1* presents the *temperature dependent dielectric permittivity* (ε^*), while *Case 2* represents the *constant dielectric permittivity* for each specified frequency, in which the value of ε^* at 25°C, calculated by equations (1) and (2), is used and assumed to be temperature independent during the process.

In addition to variation along the propagation direction, it is also seen from Fig. 4 that the maximum value of the dimensionless microwave power dissipation ($Q_{d,ave}L/Q_{0,ave}$) increases with the heating time (t) for Case 1. For example, the maximum microwave energy dissipation at a microwave power intensity ($Q_{0,ave}$) of 2.4×106 W m^{-2} for $f=0.896$ GHz, increases 35% in a 40 s heating period, 70% in 80 s, and over 100% in 120 s. The maximum microwave power dissipation for $f=2.45$ GHz increases 230% in a 60 s period during heating, while the maximum power dissipation for 10.6 and 18.0 GHz does not significantly increase with the heating time. As a result of the elevation of the temperature with time, the dielectric constant (ε') increases, which results in a decrease of the electric field (E_x). Simultaneously, the dielectric loss (ε''_{eff}) increases with the temperature. The final product of the declining electric field potential (E_x) and the increase of the dielectric loss (ε''_{eff}) augments the microwave power dissipation as the temperature rises. For Case 2, the microwave power dissipation does not vary with the heating time since dielectric permittivity is specified as a temperature independent constant in the process.

For the higher microwave frequencies, the microwave penetration becomes smaller regardless of how the dielectric permittivity changes. Except for the energy reflected from the front surface of the concrete, all microwave energy is absorbed in a distance less than 10 cm from the front surface for $f=10.6$ GHz and less than 5 cm for $f=18.0$ GHz. Variation of the dielectric permittivity changes as the temperature

Table 1. Values of the ordinary concrete properties

Properties	Density (ρ) [kg m^{-3}]	Specific heat (C_p) [J kg^{-1} K^{-1}]	Thermal conductivity (k) [W m^{-1} K^{-1}]	Compressive strength (σ_c) [MPa]	Tensile strength (σ_t) [MPa]
Reference	[27]	[28]	[28]	[18]	[18]
Values	2300	650	0.87	~50	3.5–5.0

Table 2. Thermal properties of liquid, vapor, and air

Properties	Formulation
Saturation pressure (P_s), [22]	$\ln(P_s/P_c) = \frac{T_c}{T}[a(1-T_r)+b(1-T_r)^{1.5}+c(1-T_r)^3+d(1-T_r)^6]$
	$T_r = T/T_c$, $P_c = 22.07\,\text{MPa}$, $T_c = 647.7\,\text{K}$,
	$a = -7.7645$, $b = 1.45938$, $c = -2.7758$ and $d = -1.23303$
Liquid density (ρ_l), [22]	$\frac{1}{\rho_l} = \frac{1}{\rho_s}\left(1 - c\ln\frac{\beta+P_l}{\beta+P_s}\right)$
	$\frac{\beta}{P_c} = -1+a(1-T_r)^{1/3}+b(1-T_r)^{2/3}+d(1-T_r)+e(1-T_r)^{4/3}$
	$\frac{1}{\rho_s} = \frac{R_2T_c}{P_c}Z_{RA}^{1+(1-T_r)^{2/7}}$
	$Z_{RA} = 0.2338$, $a = -9.070217$, $b = 62.46326$, $c = 0.099418$, $d = -135.1102$, $e = 157.7869$
Water latent heat (Δh_v), [22]	$\frac{\Delta h_v}{R_2T} = 7.08(1-T_r)^{0.354}+3.767(1-T_r)^{0.456}$
Vapor density (ρ_2), [29]	$P_2 = \frac{\rho_2R_2T}{1-b\rho_2}e^{-(a\rho_2/R_2T)}$
	$a = 2.19172\times10^3\,\text{Pa m}^6\,\text{kg}^{-2}$, $b = 1.8318\times10^{-3}\,\text{m}^3\,\text{kg}^{-1}$
Air density (ρ_3)	$\rho_3 = R_3T/P_3$

varies, but the microwave power dissipation barely changes in these small regions.

4.2. *Temperature and pressure distributions*

The temperature and inner pressure distributions and their variations within the concrete are dependent on the microwave power dissipation. For a 0.6 m thick concrete slab at a certain power intensity ($Q_{0,ave} = 2.4\times10^6\,\text{W m}^{-2}$), the temperature and pressure distributions and their variations with the heating time for both cases, *temperature dependent* (Case 1) and *constant* (Case 2) dielectric permittivities are plotted in Figs. 5 and 6.

Figure 5 illustrates that the temperature distribution for different frequencies is similar to the microwave power dissipation ($Q_{d,ave}L/Q_{0,ave}$) at the same frequency. For low frequencies ($f = 0.896$ and 2.45 GHz), as time elapses, the temperature and pressure anywhere within the concrete rise almost proportionally, while the differences between Case 1 and Case 2 are increasingly evident for low frequencies; see Figs. 5(a) and (b). For higher frequencies ($f = 10.6$ and 18.0 GHz), these differences are not as evident as those for the low frequencies, similar to the microwave power dissipations; see Figs. 5(c) and (d). At low frequencies ($f < 2.45$ GHz), as the dielectric permittivity varies with temperature, the temperature of Case 1 is significantly higher than that of Case 2. However, at high frequencies, the temperature distributions are very close for both cases. The variation of the power dissipation due to the variation of the dielectric permittivity initiates a greater rise in temperature.

As a result of the microwave power dissipations and the rise in the temperature distributions, the inner pressure distributions for low frequencies ($f = 0.896$ and 2.45 GHz) ascend to a higher level, see Figs. 6(a) and (b). When the heating time increases, the pressures for Case 1 become greater than that for Case 2. For higher frequencies ($f = 10.6$ and 18.0 GHz), the pressure distributions for both cases are almost identical, since the power does not differ significantly, as shown in Figs. 6(c) and (d).

For the low frequencies, as the microwave power dissipation, the temperature, and the pressure distributions of Case 1 differ from those of Case 2 in the calculation, the maximum temperature and pressure shift deeper toward the propagation direction, as seen in Figs. 5(a) and (b) and 6(a) and (b). These deeper locations of maximum temperature and pressure in the concrete slab mean that the spall-off volume will be larger than that predicted based on the constant dielectric permittivity (Case 2). Thereafter, as the dielectric permittivity varies with temperature, the actual decontamination and decommissioning process using microwave power, the frequency of which is lower than 2.45 GHz, will be shorter and the volume of the concrete spall off will be greater than that predicted by the constant dielectric model.

4.3. *Spall-off time* (t_s)

The spall-off time (t_s) is defined as the time it takes

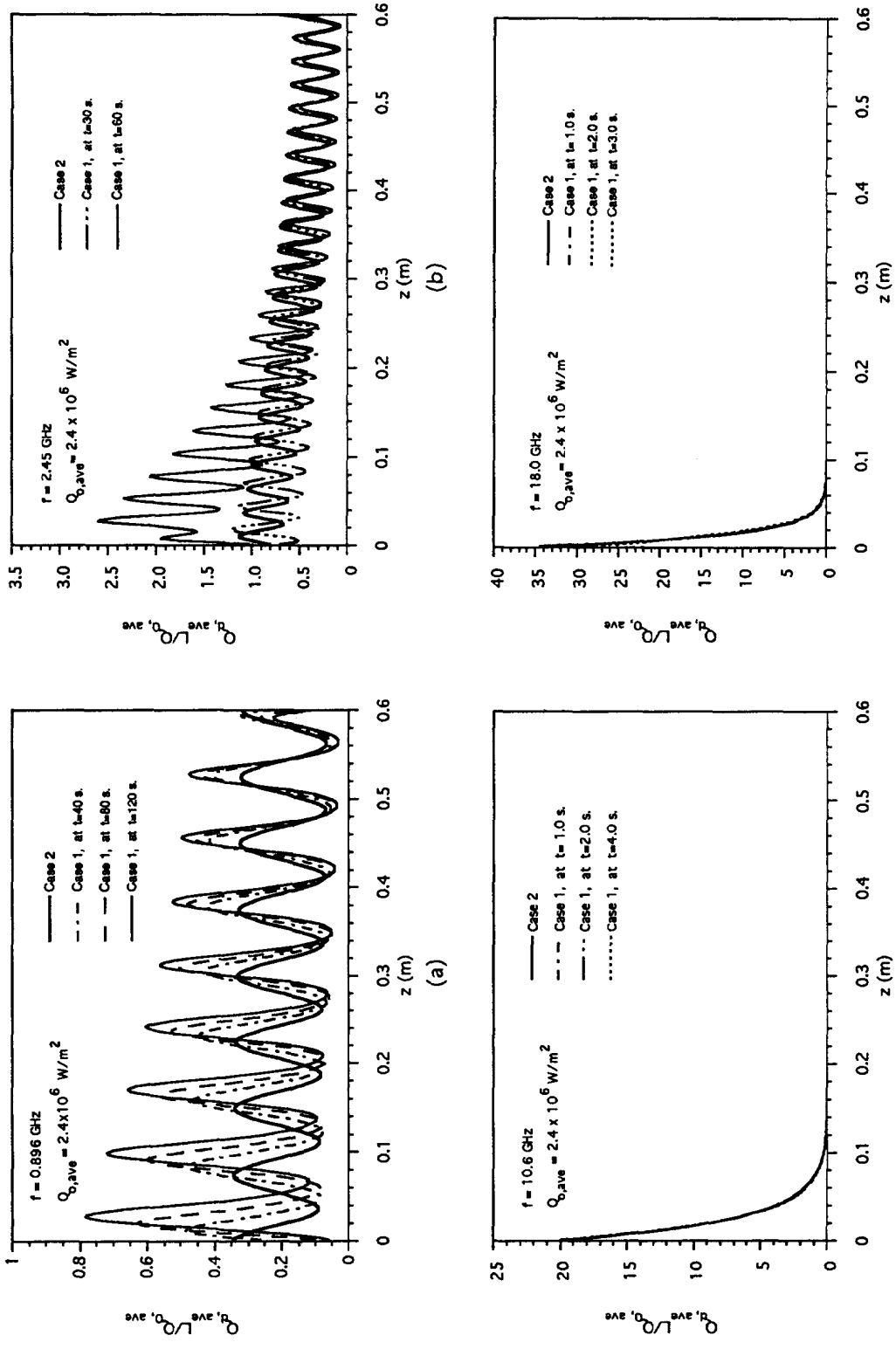

FIG. 4. Variations of the microwave power dissipation within a 0.6 m concrete slab at a microwave power intensity of 2.4×10^6 W m^{-2}. (a) Microwave power dissipation at 0.896 GHz frequency; (b) microwave power dissipation at 2.45 GHz frequency; (c) average microwave power dissipation at 10.6 GHz frequency; (d) average microwave power dissipation at 18.0 GHz frequency.

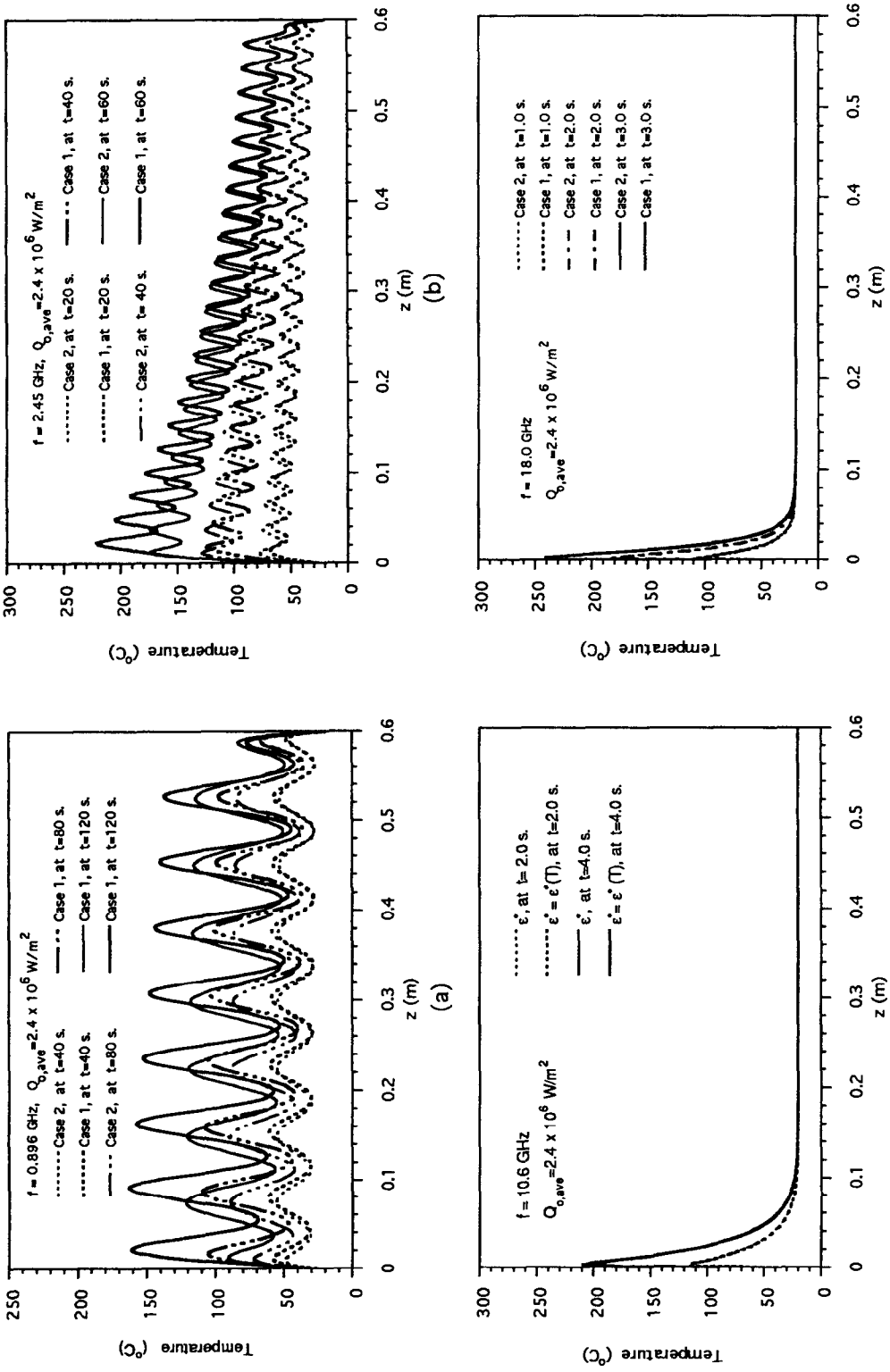

FIG. 5. Variations of the temperature distribution within a 0.6 m concrete slab at a microwave power intensity of 2.4×10^6 W m^{-2} for $\phi = 0.1$. (a) For a microwave frequency of 0.896 GHz; (b) for a microwave frequency of 2.45 GHz; (c) for a microwave frequency of 10.6 GHz; (d) for a microwave frequency of 18.0 GHz.

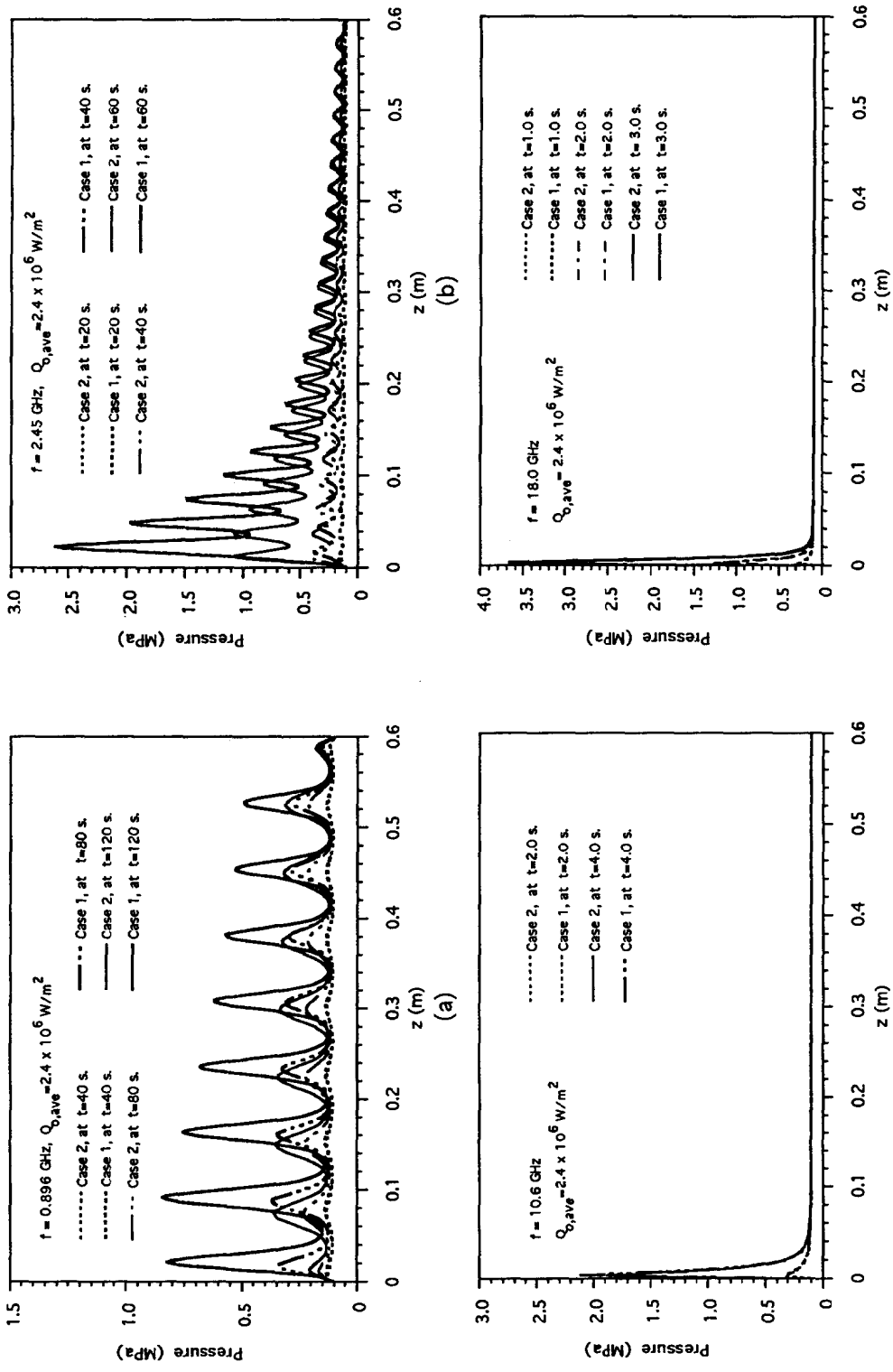

FIG. 6. Variations of the pressure distribution within a 0.6 m concrete slab at a microwave power intensity of 2.4×10^6 W m^{-2} for $\phi = 0.1$. (a) For a microwave frequency of 0.896 GHz; (b) for a microwave frequency of 2.45 GHz; (c) for a microwave frequency of 10.6 GHz; (d) for a microwave frequency of 18.0 GHz.

Table 3. Spall-off time (t_s) for different microwave power intensities ($Q_{0,ave}$) and frequencies (f)

	$Q_{0,ave}$ [W m^{-2}]											
	6.0×10^6			4.2×10^6			2.4×10^6			6.0×10^5		
f [GHz]	Case 1†	Case 2‡	diff. [%]§	Case 1	Case 2	diff. [%]	Case 1	Case 2	diff. [%]	Case 1	Case 2	diff. [%]
0.896	66.97	106.10	58.4	97.21	++‖		++	++		++	++	
2.45	25.14	33.83	34.53	36.43	48.91	34.26	65.62	90.61	30.09	++	++	
10.6	1.84	1.91	3.81	2.68	2.76	3.18	4.87	5.03	3.33	23.06	23.86	3.48
18.0	1.04	1.11	6.31	1.53	1.59	3.85	2.82	2.99	5.99	14.17	15.08	6.44

† Case 1. Model using temperature dependent dielectric permittivity; the values are described by equations (1) and (2).
‡ Case 2. Model using constant dielectric permittivity; the values measured at 25°C for different frequencies are used.
§ diff. (t_s for Case 1 $-$ t_s for Case 2)/t_s for Case 1 $\times$ 100%.
‖ ++ t_s longer than 120 s.

the inner pressure (P) to equal the concrete tensile strength (σ_t = 4.0 MPa) during the process. The spall-off times for both cases at different microwave frequencies (f) and microwave intensities ($Q_{0,ave}$) are listed in Table 3. Practically, when the spall-off time is close to two minutes, the escape of the moisture or steam and air will dramatically reduce the maximum inner pressure within the concrete slab. Therefore, a limit of the spall-off time is set to 120 s in the analysis.

It is seen from Table 3 that for f = 0.896 GHz with $Q_{0,ave} = 6.0\times10^6$ W m^{-2}, the spall-off time (t_s) has the greatest difference (58.44%) between Case 1 and Case 2. For f = 2.45 GHz, the spall-off time for Case 1 is about 35% less than that of Case 2 at a microwave power intensity ($Q_{0,ave}$) ranging from 2.4 to 6.0×10^6 W m^{-2}. For higher frequencies, for example, f = 10.6 and 18.0 GHz, the spall-off time at all microwave power intensities ranging from 6.10×10^5 to 6.0×10^6 W m^{-2} for both cases does not differ too much, only 3–6%, which has the same tendency as the power dissipation, the temperature, and the pressure distributions.

For the low frequency (f < 2.45 GHz), as the dielectric permittivity varies with temperature, the power dissipation increases. Therefore, the maximum temperature and pressure are essentially increased, which finally results in a shorter spall-off time (t_s), compared to the model of constant dielectric properties. For a higher microwave frequency (f > 10.6 GHz), the maximum temperature and pressure are very close for both cases since microwave power dissipation within the concrete is not affected, whether or not the dielectric permittivity varies with temperature. Thus, this makes the concrete spall-off time for both models the same.

5. CONCLUDING REMARKS

The effects of the variation of the dielectric properties with temperature on the power dissipation distribution within the concrete ($Q_{d,ave}$), the temperature (T), the pressure distributions (P) and their variations with the microwave heating time are fully discussed. The spall-off times (t_s) for both temperature dependent and constant dielectric permittivity (ε^*) models at different microwave power intensities ($Q_{0,ave}$) and frequencies (f) are also discussed. Based on these discussions, the following facts are concluded.

(1) For a low microwave frequency (f < 2.45 GHz), as the complex dielectric permittivity (ε^*) increases with temperature, the total power dissipation and the maximum value of this dissipation within the concrete increases significantly. This power increase due to the variation of ε^* accelerates the temperature rise. For a high microwave frequency (f > 10.6 GHz), the power dissipation and its maximum value barely change, since the penetration of the high microwave frequencies is low.

(2) As a result of the ε^* variation, location of the maximum power dissipation, the temperature, and the pressure slowly shift deeper towards the propagation direction. This shift should cause more contaminated concrete to spall off.

(3) As ε^* increases with temperature, the temperature and pressure distributions for a low frequency (f < 2.45 GHz) change vitally as the microwave power dissipation did. Increase in the power dissipation initiates a higher temperature, and especially originates a higher maximum temperature and pressure compared with the model of a constant ε^*. For a high frequency (f > 10.6 GHz), the temperature and pressure distributions exhibit no such difference when microwave power dissipations for both models are almost the same.

(4) For the model of temperature dependent dielectric properties, at a low frequency (f < 2.45 GHz), the spall-off time (t_s) is less than that predicted by constant dielectric properties. For example, at f = 0.896 GHz, the spall-off time (t_s) calculated by the temperature dependent model is about 55% shorter, and at f = 2.45 GHz, it is 35% shorter, compared to the constant dielectric properties model. For a higher frequency (f > 10.6 GHz), the spall-off time for the two models has only about a 3–6% difference.

(5) Generally, the effect of the variation of the concrete dielectric properties with temperature should be considered in the theoretical modeling, and especially for a low frequency ($f < 2.45$ GHz), the variation of the dielectric properties must be incorporated.

Acknowledgement—The results presented in this paper were obtained in the course of research sponsored by the Department of Energy under Subcontract No. DE-AC05-840R21400.

REFERENCES

1. E. C. Okress *Microwave Power Engineering*, Vol. 2. Academic Press, New York (1968).
2. D. A. Copson, *Microwave Heating*, (2nd Edn). AVI, Westport, Connecticut (1975).
3. W. R. Tinga and S. O. Nelson, Dielectric properties of materials for microwave processing—tabulated, *J. Microwave Power* **8**(1), 23–65 (1973).
4. P. W. McMillian and G. Partridge, The dielectric properties of certain $Zn\text{-}Al_2\text{-}O_3\text{-}SiO_2$ glass ceramics, *J. Mat. Sci.* **7**, 847 (1972).
5. A. Watson, *Microwave Power Engineering*, Vol. 2. Academic Press, New York (1968).
6. H. Yasunaka, M. Shibamoto and T. Sukagawa, Microwave decontaminator for concrete surface decontamination in JPDR, *Proceedings of the Int. Decommissioning Symposium*, pp. 109–115 (1987).
7. D. L. Hills, The removal of concrete layers from biological shields by microwave, *EUR* 12185, Nuclear Science and Technology Commission of the European Communities (1989).
8. T. L. White, R. G. Grubb, L. P. Pugh, D. Foster, Jr. and W. D. Box, Removal of contaminated concrete surfaces by microwave heating—phase I results, *Waste Management 92, Proceedings of 18th American Nuclear Society on Waste Management*, Tucson, Arizona (1992).
9. W. Li, M. A. Ebadian, T. L. White and R. G. Grubb, Heat and mass transfer in a contaminated porous concrete slab subjected to microwave heating. In *General Papers in Heat Transfer and Heat Transfer in Hazardous Waste Processing*, HTD-Vol. 212, pp. 143–153 (1992).
10. W. Li, M. A. Ebadian, T. L. White and R. G. Grubb, Heat transfer within a radioactive contaminated concrete slab applying a microwave heating technique, *J. Heat Transfer* **115**, 42–50 (1993).
11. A. V. Luikov, *Heat and Mass Transfer in Capillary-Porous Bodies* (1st English Edn). Pergamon, New York (1966).
12. T. Z. Harmathy, Simulations moisture and heat transfer in porous systems with particular reference to drying, *I & EC Fund.* **8**, 92 (1969).
13. C. D. L. Huang, H. H. Siang and C. H. Best, Heat and moisture transfer in concrete slab, *Int. J. Heat Mass Transfer* **22**, 257–266 (1979).
14. C. K. Wei, H. T. Davis, E. A. Davis and J. Gordon, Heat and mass transfer in water-laden sandstone: convective heating, *A.I.Ch.E. Jl* **31**(8), 1338–1348 (1985).
15. S. Whitaker, A theory of drying in porous media, *Adv. Heat Transfer* **13**, 119–203 (1977).
16. C. K. Wei, H. T. Davis, E. A. Davis and J. Gordon, Heat and mass transfer in water-laden sandstone: microwave heating, *A.I.Ch.E. Jl* **31**(5), 842–848 (1985).
17. M. A. Ebadian and W. Li, Concrete decontamination and decommissioning by using microwave technology, *Final Report*, DOE research grant #DE-AC05-840R21400 (1992).
18. A. M. Neville, *Properties of Concrete* (3rd Edn). Pitman, Massachusetts (1981).
19. D. Misra, A quasi-static analysis of open-ended coaxial lines, *IEEE Trans., Microwave Theory and Techniques* **MTT-35**, 925 (1987).
20. D. Misra, M. Chabbra, B. R. Epstein, M. Mirotznik and K. Foster, Noninvasive electrical characterization of materials at microwave frequencies using open-ended coaxial line: test of an improved calibration technique, *IEEE Trans., Microwave Theory Techniques* **38**, 8 (1990).
21. J. B. Hasted and M. A. Shah, Microwave absorption by water in building material, *Brit. J. Appl. Phys.* **15**, 825–836 (1964).
22. R. C. Reid, J. M. Prausnitz and R. E. Poling, *The Properties of Gases and Liquids* (4th Edn). McGraw-Hill, New York (1987).
23. L. Haar, J. S. Gallagher and G. S. Kell, *NBS/NRC Steam Tables*. Hemisphere, New York (1984).
24. C. T. A. Johnk, *Engineering Electromagnetic Fields and Waves* (2nd Edn). Wiley, New York (1988).
25. M. F. Iskander, *Electromagnetic Fields and Waves*. Prentice Hall, New Jersey (1992).
26. O. A. Liskovets, The method of lines (reviews), *Diff. Eqns* **1**, 1308 (1965).